J. Phys. Chem. A **2003,** *107,* 10435−10440 **10435**

Direct ab Initio Dynamics Study of the Reaction of the Hydrogen Atom with Formyl Chloride

Qian Shu Li* and Qiong Luo

School of Science, Beijing Institute of Technology, Beijing 100081, P. R. China

Received: July 15, 2003; In Final Form: September 19, 2003

A direct ab initio dynamics study is presented on two channels of the gas-phase reaction of the hydrogen atom with formyl chloride, HCOCl. The geometries, harmonic vibrational frequencies, energies, and enthalpies of all of the stationary points are calculated at the BHandHLYP, MP2, and QCISD levels of theory with the cc-pVDZ basis set. The minimum energy paths (MEPs) of both channels of the title reaction are also computed with the same methods and basis set. The energies of stationary points and the points along the MEP for each channel are refined by means of some single-point multilevel energy calculations (HL). The rate constants are evaluated with the conventional transition state theory (TST), the improved canonical varitional transition state theory (ICVT), and the improved canonical varitional transition state theory with small-curvature tunneling correction (ICVT/SCT) in the temperature range of 300−2500 K. The fitted Arrhenius expressions of the calculated ICVT/SCT rate constants at the HL//BHandHLYP/cc-pVDZ and HL//QCISD/cc-pVDZ levels of theory are $k_1^{\mathrm{ICVT/SCT}}(T) = 1.16 \times 10^{-19}\ T^{2.61}\ \mathrm{e}^{(-1018.4/T)}$ and $k_1^{\mathrm{ICVT/SCT}}(T) = 1.64 \times 10^{-18}\ T^{2.25}\mathrm{e}^{(-1943.1/T)}$ for the H abstraction channel, and $k_2^{\mathrm{ICVT/SCT}}(T) = 1.16 \times 10^{-17}T^{1.90}\mathrm{e}^{(-3017.1/T)}$ and $k_2^{\mathrm{ICVT/SCT}}(T) = 1.85 \times 10^{-18}T^{2.12}\mathrm{e}^{(-3473.4/T)}$ for the Cl abstraction channel, respectively.

I. Introduction

As is known, the stratospheric ozone layer is of vital importance to life on Earth. Ozone depletion in the polar regions during springtime, caused by the widespread use of chlorofluorocarbons (CFCs) as refrigeration fluids,[1−7] has received great attentions from scientists. To protect the stratospheric ozone layer, hydrofluorocarbons (HFCs) and hydrochlorofluorocarbons (HCFCs) are being implemented as replacement of the CFCs.[1,5,8,9] The HFCs and HCFCs are more active than the CFCs in the troposphere[1,5,6,10] and thus are relatively innocuous in their effect on the ozone layer. So tropospheric transformation products of a series of the HFCs and HCFCs are of great interest in the research of protecting the stratospheric ozone layer.

The formyl chloride molecule plays an important role in the chemistry of the polluted troposphere. It is a transient molecule in the degradation not only of the HCFCs but also of a number of important chlorinated hydrocarbons, such as CH_3Cl, CH_2Cl_2, and $CHCl_3$[11−15] in the atmosphere, as well as from the tropospheric reaction of the Cl atom with volatile organic compounds such as isoprene.[16] The lifetime of HCOCl in the atmosphere is a critical parameter in assessing the procedure of removal of those pollutants. To estimate the lifetime, the kinetics data of different removal channels have to be considered.

Although some works have been performed to study the dynamics of the bimolecular reactions of HCOCl with Cl[17−19] or H_2O,[20] OH,[17,21,22] as well as the unimolecular decompositions,[23−25] no study was done, either experimentally or theoretically, for the reaction of HCOCl with H to the best of our knowledge. Because there are considerable organic sources for producing hydrogen atoms in the atmosphere, it is interesting to evaluate the kinetics data of the abstraction reaction of HCOCl with H and to compare it with other reactions.

In the present study, we consider two channels of the abstraction reaction of HCOCl with H:

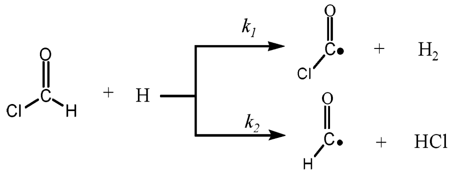

Their potential energy surface information required for the dynamical calculations is computed using density functional theory and quadratic configuration interaction theory as well as some single-point multilevel energy calculations. The direct ab initio dynamics methods employed in this study are based on an improved canonical variational transition state theory with the multidimensional centrifugal-dominant small-curvature semiclassical adiabatic ground-state tunneling correction.

II. Methodology

A. Rate Constant Calculations. The improved canonical variational transition state theory (ICVT),[26] implemented with features from microcanonical ensemble, is a modification to the canonical variational transition state theory (CVT) and more accurate than the latter for calculations of rate constants of low temperatures where the contribution from the threshold region is important. Within the framework of ICVT, the improved generalized transition state rate constant, $k^{\mathrm{IGT}}(T, s)$, can be calculated at the reaction coordinate s along the MEP at a fixed temperature; then the ICVT rate constant is obtained by

---

* To whom correspondence should be addressed. E-mail: qsli@bit.edu.cn. Fax: +86−10−68912665. Phone: +86-10-68912665.

10.1021/jp0360568 CCC: \$25.00

minimizing $k^{\mathrm{IGT}}(T, s)$ along the MEP at the given temperature as follows:

$$k^{\mathrm{ICVT}}(T) = \min_{s} k^{\mathrm{IGT}}(T, s)$$

in which

$$k^{\mathrm{IGT}}(T,s) = [h\, \phi^{\mathrm{R}}(T)]^{-1} \int_{V_{\mathrm{a}}^{\mathrm{G}}}^{\infty} \mathrm{d}E\ \mathrm{e}^{-\beta E} N^{\mathrm{GT}}(E,s)$$

where h is Planck's constant, $\phi^{\mathrm{R}}(T)$ is the reactant partition function per unit volume, $\beta = 1/(k_{\mathrm{B}}T)$, k_{B} is Boltzmann's constant, $V_{\mathrm{a}}^{\mathrm{G}}$ is the vibrationally adiabatic ground-state potential energy at s, and $N^{\mathrm{GT}}(E,s)$ is the quantized cumulative reaction probability at energy E and reaction coordinate s.

Finally, the rate constant is

$$k(T) = \kappa(T) k^{\mathrm{ICVT}}(T)$$

where $\kappa(T)$, the transmission coefficient, can be calculated by the small-curvature tunneling (SCT)[27−30] method, and the quantum effects along the reaction coordinate can be included.

It should be mentioned that the normal-mode frequency analysis failed to correctly predict the frequencies along the MEPs in this study. Thus, the redundant curvilinear reaction coordinate is adopted in the calculations of rate constants to reproduce the frequencies.[31] The rate constants of the title reaction are computed using three levels of theory, namely, the conventional transition state theory (TST), the improved canonical varitional transition state theory (ICVT), and the improved canonical varitional transition state theory with small-curvature tunneling correction (ICVT/SCT). The evaluations of all of the rate constants are performed employing the Polyrate8.2 program.[31]

B. Electronic Structure Calculations. The geometries and frequencies of all stationary points (reactants, products, and the transition states) are optimized at the BHandHLYP,[32,33] MP2,[34] and QCISD[35] levels of theory with Dunning's[36,37]correlation consistent polarized valence double-ζ basis set, namely, the cc-pVDZ basis set. Here, BHandHLYP presents the combination of Becke's half and half (BHandH) nonlocal exchange functional with Lee−Yang−Parr (LYP) correlation functionals. MP2 denotes the second-order Möler−Plesset perturbation theory with frozen core approximation. QCISD stands for the quadratic configuration interaction theory with all single and double substitutions. To yield a more reliable reaction enthalpy and barrier height, single-point calculations for all stationary points are further refined by means of some single-point multilevel energy calculations (HL) based on the optimized geometries at the BHandHLYP/cc-pVDZ, MP2/cc-pVDZ, and QCISD/cc-pVDZ levels of theory. The HL method employs a combination of QCISD(T) and MP2,[38] and calculations can be expressed as

$$\begin{aligned} E_{\mathrm{HL}} = {} & E[\mathrm{QCISD(T)/cc\text{-}pVTZ}] + \{E[\mathrm{QCISD(T)/cc\text{-}pVTZ}] - \\ & E[\mathrm{QCISD(T)/cc\text{-}pVDZ}]\}\ 0.46286 + E[\mathrm{MP2/cc\text{-}pVQZ}] + \\ & \{E[\mathrm{MP2/cc\text{-}pVQZ}] - E[\mathrm{MP2/cc\text{-}pVTZ}]\}\ 0.69377 - \\ & E[\mathrm{MP2/cc\text{-}pVTZ}] - \{E[\mathrm{MP2/cc\text{-}pVTZ}] - \\ & E[\mathrm{MP2/cc\text{-}pVDZ}]\}\ 0.46286 \end{aligned}$$

Here QCISD(T)/cc-pVTZ is referred to as the quadratic configuration interaction calculation including single and double substitutions with a triples contribution to the energy added,[35] using Dunning's correlation consistent polarized valence triple-ζ basis set.[37] The cc-pVQZ is Dunning's correlation consistent polarized valence quadruple-ζ basis set.[37]

For convenience, these methods for energy refinement are denoted as HL//BHandHLYP, HL//MP2, and HL//QCISD, respectively. All of the electronic structure calculations are carried out using the Gaussian 98 program.[39]

III. Results and Discussion

A. Stationary Points. A pictorial of the optimized geometries and the calculated geometric parameters of the equilibrium and transition states of the two channels is displayed in Figure 1 along with the available experimental data.[40−42] For HCOCl, all of the predicted bond angles are prettily close to the available experimental data. The C−H and C−Cl bond lengths at the BHandHLYP/cc-pVDZ level are closer to the experimental data than those at the MP2/cc-pVDZ and QCISD/cc-pVDZ levels. When it comes to the C−O bond lengths, the MP2/cc-pVDZ and QCISD/cc-pVDZ levels of theory nearly iterate the experimental data with the BHandHLYP/cc-pVDZ level of theory having the difference of 0.02 Å. In general, all of the three methods adopted in the present calculations can provide a reasonable structure for HCOCl compared to the experimental data[42] and previous high-level theoretical results.[43,44] As can be seen from Figure 1, the predicted geometries of both transition states (TS_1 and TS_2) are in good agreement between all of the levels of theory. The lengths of all of the active bonds, C−H and H−H of TS_1 as well as C−Cl and H−Cl of TS_2, from the BHandHLYP/cc-pVDZ method are quite close to those from the QCISD/cc-pVDZ method. For the products, the structures predicted by the three methods are quite consistent and in good agreement with the experimental data.[40,41] In a word, all three methods agree well in predicting geometries for the stable structures and the transition states of the current two channels.

Table 1 lists the harmonic vibrational frequencies and the zero point energies of the equilibrium and transition states employing the BHandHLYP, MP2, and QCISD levels of theory with the same basis set cc-pVDZ along with the available experimental data.[20,45−53] For the HCOCl and products, the computed frequencies from different levels are consistently slightly larger than the experimental values, except for the COCl at the QCISD/cc-pVDZ level, with the largest discrepancy of 12%. For both transition states (TS_1 and TS_2), the predicted values of imaginary frequencies from the BHandHLYP/cc-pVDZ method are the smallest, whereas the MP2/cc-PVDZ method provides the largest imaginary frequencies. The value of the imaginary frequency of TS_1 is larger than that of TS_2 at all three levels of theory. The reason is simply because the vibration involved in TS1 primarily involves a hydrogen, whereas that in TS2 involves a chlorine. In the basis of the mass difference of the atoms involved, it could be expected that the tunneling effect would be more important in a process involving only hydrogen than one involving a chlorine. From the data in Table 1, it can be seen that the BHandHLYP/cc-pVDZ method can give a reasonable prediction for vibrational frequencies and is comparable to the QCISD/cc-pVDZ method for the present reaction.

The reaction energies (ΔV), the classical potential barriers ($V^{\ddagger}$), the vibrationally adiabatic ground-state potential ($V_{\mathrm{a}}^{\mathrm{G}}$), and the reaction enthalpies ($\Delta H^{\circ}_{298\mathrm{K}}$) are listed in Table 2. Note that the values of $V^{\ddagger}$ and $V_{\mathrm{a}}^{\mathrm{G}}$ are calculated at the corresponding saddle points. For the H abstraction channel, the refined reaction enthalpies are −15.39, −15.29, and −14.70 kcal mol^{-1} at the QCISD(T)/cc-pVTZ level of theory and are −14.76, −14.88, and −14.25 kcal mol^{-1} at the HL level of theory, respectively, based on the geometries optimized at the QCISD/

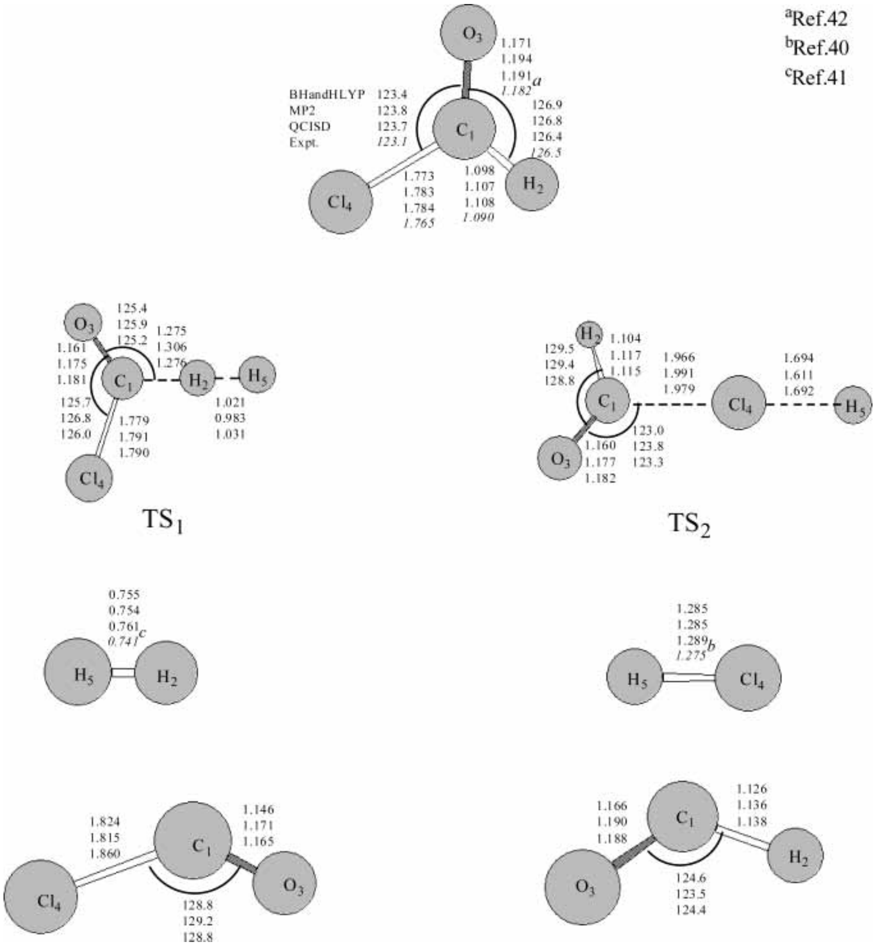

Figure 1. Pictorial of optimized geometries of the stationary points.

TABLE 1: Harmonic Vibrational Frequencies (cm^{-1}) and Zero-Point Energy (kcal mol^{-1}) of the Reactant, Products, and Transition States Using the Three Methods with the Same Basis Set cc-pVDZ

species	methods	frequencies									ZPE
HCOCl(C_s)	BHandHLYP	476	767	994	1369	1953	3164				12.47
	MP2	460	750	955	1350	1816	3112				12.07
	QCISD	464	755	955	1354	1848	3094				12.11
	expt	457^{a,b}	738.8^{a,b}	932^{a,c}	1307^{a,d}	1784^{a,e}	2929.18^{a}				
COCl(C_s)	BHandHLYP	334	594	2058							4.27
	MP2	371	635	1959							4.24
	QCISD	287	553	1928							3.96
	expt	334.6^{f}	570.1^{g}	1884^{h}							
H_2($D_{\infty h}$)	BHandHLYP	4478									6.40
	MP2	4501									6.43
	QCISD	4383									6.26
	expt^{j}	4401									
TS1(C_s)	BHandHLYP	298	332	454	695	1116	1280	1372	2020	1652i	10.82
	MP2	306	334	440	684	1143	1282	1416	2223	2215i	11.20
	QCISD	290	330	444	687	1090	1276	1350	1904	1887i	10.54
HCO(C_s)	BHandHLYP	1139	2043		2747						8.48
	MP2	1124	1942		2712						8.26
	QCISD	1135	1893		2675						8.15
	expt^{k}	1076.5	1858		2442						
HCl($C_{\infty v}$)	BHandHLYP	3041									4.35
	MP2	3075									4.40
	QCISD	3031									4.33
	expt^{j}	2991									
TS2(C_s)	BHandHLYP	259	308	424	693	852	1242	2013	3080	978i	12.69
	MP2	264	334	439	716	838	1214	2131	3005	1460i	12.76
	QCISD	264	301	408	667	819	1233	1886	3011	1131i	12.28

[a] Reference 20. [b] Reference 47. [c] Reference 45. [d] Reference53. [e] Reference 46. [f] Reference 49. [g] Reference48. [h] Reference 50. [j] Reference 52. [k] Reference 51.

cc-pVDZ, BHandHLYP/cc-pVDZ, and MP2/cc-pVDZ levels of theory, whereas the corresponding difference between the data from the QCISD(T) and HL levels of theory are 0.63, 0.41, and 0.45 kcal mol^{-1}. It is obvious that the reaction enthalpies calculated at the QCISD(T)//QCISD (HL//QCISD) and QCISD(T)//BHandHLYP ((HL//BHandHLYP) levels of theory are very

TABLE 2: Reaction Energetic Parameters (kcal mol^{-1}) at Different Levels of Theory

method	ΔV^a	$V^{\ddagger\,b}$	$V_a^{G\,b}$	ΔH°_{298K} ^{c}
$CHClO + H \rightarrow COCl + H_2$				
BHandHLYP/cc-pVDZ	−11.70	5.78	4.13	−14.60
MP2/cc-pVDZ	−7.63	12.80	11.94	−9.79
QCISD/cc-pVDZ	−12.73	9.41	7.57	−15.77
QCISD(T)/cc-pVTZ//BHandHLYP/cc-pVDZ	−12.39	8.32	6.67	−15.29
QCISD(T)/cc-pVTZ//MP2/cc-pVDZ	−12.54	8.05	7.17	−14.70
QCISD(T)/cc-pVTZ//QCISD/cc-pVDZ	−12.35	8.26	6.69	−15.39
HL//BHandHLYP/cc-pVDZ	−11.98	8.12	6.47	−14.88
HL//MP2/cc-pVDZ	−12.09	7.81	6.93	−14.25
HL//QCISD/cc-pVDZ	−11.72	8.09	6.52	−14.76
$CHClO + H \rightarrow HCO + HCl$				
BHandHLYP/cc-pVDZ	−23.10	10.26	10.48	−22.03
MP2/cc-pVDZ	−16.70	19.76	20.47	−15.17
QCISD/cc-pVDZ	−23.18	14.36	14.52	−22.08
QCISD(T)/cc-pVTZ//BHandHLYP/cc-pVDZ	−21.73	10.94	11.15	−20.66
QCISD(T)/cc-pVTZ//MP2/cc-pVDZ	−21.75	10.27	10.98	−20.22
QCISD(T)/cc-pVTZ//QCISD/cc-pVDZ	−21.70	10.96	11.13	−20.60
HL//BHandHLYP/cc-pVDZ	−21.44	9.64	9.85	−20.37
HL//MP2/cc-pVDZ	−21.45	8.64	9.35	−19.92
HL//QCISD/cc-pVDZ	−21.38	9.70	9.87	−20.28

[a] Reaction energy without zero-point energy correction. [b] The $V^{\ddagger}$ and V_a^G are calculated at the corresponding saddle point. [c] Reaction enthalpy at 298 K.

close with the difference of only 0.1 (0.12) kcal mol^{-1}; the QCISD(T)//MP2 (HL//MP2) overestimates the reaction enthalpy compared to the QCISD(T)//QCISD method. This difference in reaction enthalpy may primarily come from the difference in geometries of the transition state, where the active bonds optimized at the QCISD/cc-pVDZ and BHandHLYP/cc-pVDZ levels of theory are close compared to those optimized at the MP2/cc-pVDZ level of theory. The pre-refined reaction enthalpies calculated at the BHandHLYP/cc-pVDZ and QCISD/cc-pVDZ levels of theory are also quite good with the difference smaller than 1 (1.01) kcal mol^{-1} compared to the refined enthalpies from the QCISD(T) (HL) level of theory. However, MP2/cc-pVDZ provides a bad estimation for the reaction enthalpy. The same trend also appears in the vibrationally adiabatic ground-state potentials. For the Cl abstraction channel, compared to the refined enthalpy from the QCISD(T)//QCISD (HL//QCISD) level of theory, the result provided by MP2/cc-pVDZ has the largest discrepancy of 5.43 (5.11) kcal mol^{-1}, whereas QCISD(T)//BHandHLYP (HL//BHandHLYP) affords good result with the difference of only 0.06 (0.38) kcal mol^{-1}. Briefly, it can be pointed out that the BHandHLYP/cc-pVDZ and QCISD/cc-pVDZ levels provide resonable geometric information, and additional single-point HL calculations are needed to get accurate energetic information. Unfortunately, there are no available experimental data for comparison. It may be suggested that the energetic information obtained at the HL//BHandHLYP and HL//QCISD levels of theory are relatively reliable.

As can be seen from Table 2, it is obvious that the barrier heights of the H abstraction channel are smaller than those of the Cl abstraction channel at all of the three levels of theory, respectively. Consequently, it could be anticipated that the rate constant of the H abstraction channel will be larger than those of the Cl abstraction channel.

B. Reaction Path Properties. The MEPs from $s = -1.50$ to $+1.50$ (amu)$^{1/2}$ bohr, done in the mass weighted Cartesian coordinate with a step size of 0.01 amu$^{1/2}$ bohr using the intrinsic reaction coordinate (IRC) method,[54] are obtained at the BHandHLYP/cc-pVDZ, MP2/cc-pVDZ, and QCISD/cc-pVDZ levels of theory. Furthermore, at 20 selected points (10 points in the reactant channel and 10 points in the product channel) along the MEP, the Hessian matrixes and the harmonic vibrational frequencies are obtained. Then the energies are recalculated along the MEPs at the HL level of theory. The variational transition state theory with interpolated single-point energies (VTST-ISPE)[31] method is used for interpolating information along the MEPs.

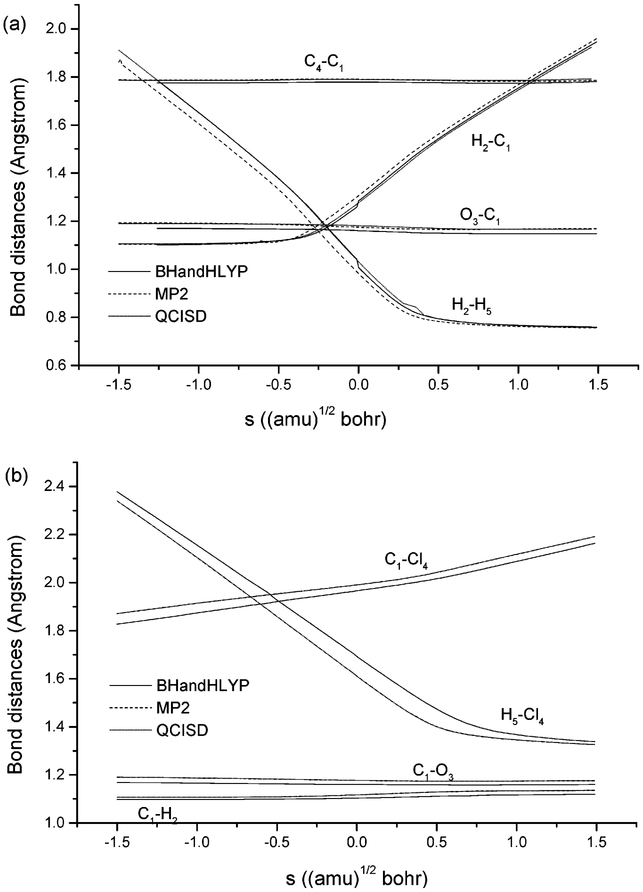

Figure 2. Bond distance curves of the reaction as functions of the reaction coordinate *s* at the BHandHLYP/cc-pVDZ, MP2/cc-pVDZ, and QCISD/cc-pVDZ levels of theory. (a) The H abstraction channel. (b) The Cl abstraction channel.

Figure 2 displays how bond-lengths vary as functions of the reaction coordinates at the BHandHLYP/cc-pVDZ, MP2/cc-pVDZ, and QCISD/cc-pVDZ levels of theory. It can be seen that the curves of each bond obtained by different calculation methods nearly overlap. For the H abstraction channel, it is seen from Figure 1a that the change of the H_2-C_1 bond length remains insensitive up to $s = -0.3$amu$^{1/2}$ bohr and then increases smoothly afterward with the increase of the IRC coordinate. However, the H_2-H_5 bond length decreases smoothly to the H−H bond distance of 0.76 Å at $s = 0.6$ amu$^{1/2}$ bohr. This means that the synergetic process of forming the H_2-H_5 bond and breaking the H_2-C_1 bond of the H abstraction channel takes place in the region, $s = -0.3\sim0.6$ amu$^{1/2}$ bohr along the MEP. For the Cl abstraction channel, the variation of the Cl_4-C_1 bond distance is very mild along the whole MEP compared to the H_2-C_1 bond of the H abstraction channel. As shown in Figure 1b, the HCl is formed at $s = \sim0.75$ amu$^{1/2}$ bohr.

The classical potential energy curves (V_{MEP}) and vibrationally adiabatic ground-state potential energy curves (V_a^G) of both channels as functions of the reaction coordinate *s* are presented in Figure 3 at the HL level of theory. It is clear that both reaction channels undergo an elementary reaction process. Around the

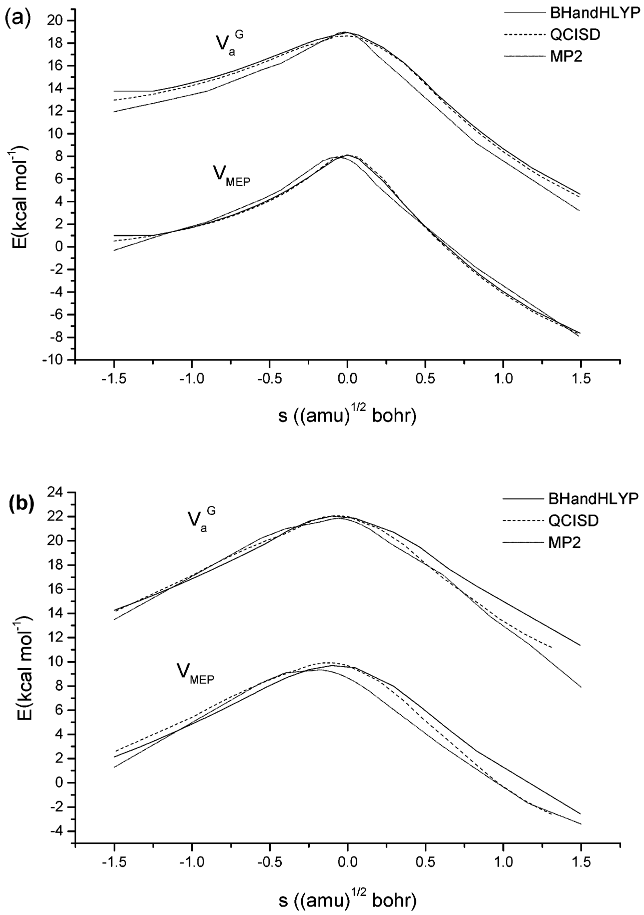

Figure 3. Classical potential energy (V_{MEP}) and the ground state vibrationally adiabatic potential energy (V_a^G) curves of the reaction as functions of the reaction coordinate *s* at the HL//BHandHLYP, HL//MP2, and HL//QCISD levels of theory. (a) The H abstraction channel. (b) The Cl abstraction channel.

top of V_{MEP} and V_a^G , the curves of the Cl abstraction channel are slightly flatter than those of the H abstraction channel, which may result in a stronger quantum transmission effect of the H abstraction channel than that of the Cl abstraction channel.

C. Rate Constant Calculations. Because the energetic information provided by the HL//MP2 level of theory is unsatisfactory compared to those by the HL//BHandHLYP and QCISD(T)//QCISD levels of theory, here only the TST, ICVT, and ICVT/SCT rate constants calculated at the HL//BHandHLYP and HL//QCISD levels of theory are discussed for both the H abstraction and the Cl abstraction channels in the temperature range of 300−2500 K. It should be pointed out that the symmetry numbers of both channels of the title reaction are equal to 1. The three-parameter Arrhenius expressions of the calculated ICVT/SCT rate constants, $k_1^{ICVT/SCT}(T) = 1.16 \times 10^{-19}\ T^{2.61}e^{(-1018.4/T)}$ and $k_1^{ICVT/SCT}(T) = 1.64 \times 10^{-18}\ T^{2.25}e^{(-1943.1/T)}$ for the H abstraction channel and $k_2^{ICVT/SCT}(T) = 1.16 \times 10^{-17}T^{1.90}e^{(-3017.1/T)}$ and $k_2^{ICVT/SCT}(T) = 1.85 \times 10^{-18}T^{2.12}e^{(-3473.4/T)}$ for the Cl abstraction channel, are fitted at the HL//BHandHLYP/cc-pVDZ and HL//QCISD/cc-pVDZ levels of theory, respectively. Figure 4 shows the Arrhenius plots calculated from the HL//BHandHLYP and HL//QCISD methods vs the temperatures.

For the H abstraction channel, it can be found that the four curves of the TST and ICVT rate constants at both theory levels are quite close, indicating that the variational effects on the calculation of rate constants are small for the reaction. The ICVT/SCT rate constants are consistently larger than the ICVT rate constants with the $k_1^{ICVT/SCT}/k_1^{ICVT}$ factors of 1.08 and 1.06 at 2500 K at the HL//BHandHLYP and HL//QCISD levels of theory, respectively, and the corresponding factors increase to 37.2 and 25.5 at 300 K. This trend is quite obvious in Figure 4a. The results tally with the character of the H transfer reaction, namely, the tunneling effect is crucial in the H transfer reaction. Similarly to the H abstraction channel, the variational effect on the calculation value of rate constant may be ignored for the Cl channel. However, the tunneling effects for this channel are rather slender at the HL//BHandHLYP level and nearly disappear at the HL//QCISD level (see Figure 4b).

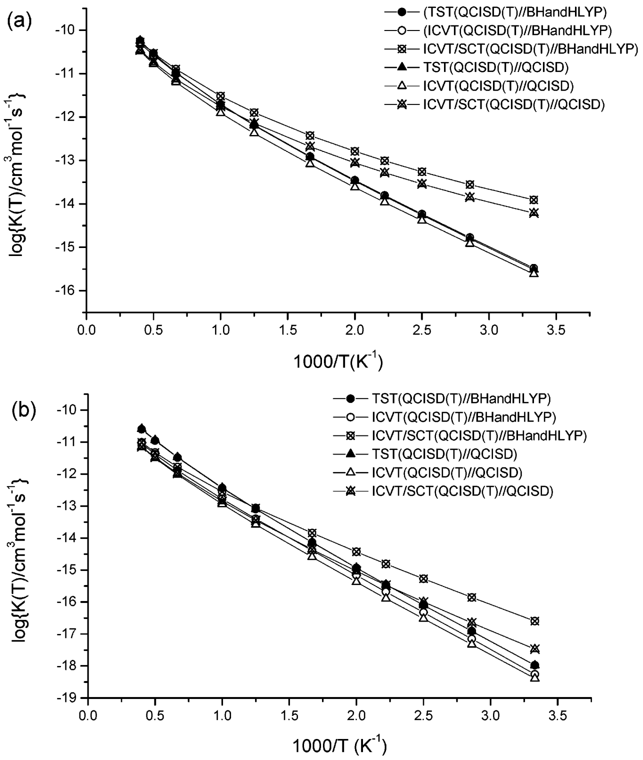

Figure 4. Calculated Arrhenius plots of the rate constants at the HL//BHandHLYP and HL//QCISD levels of theory of the reaction vs 1000/*T*(K^{-1}). (a) The H abstraction channel. (b) The Cl abstraction channel.

From our calculations, the rate constant k_1 is consistently larger than the rate constant k_2 and the difference between k_1 and k_2 increases with the decrease of the temperatures. From 300 to 2500 K, the ranges of the factor of $k_1^{ICVT/SCT}/k_2^{ICVT/SCT}$ are about 5 × 10^2∼2 and 7 × 10∼4 at the HL//BHandHLYP and HL//QCISD levels of theory, respectively. As a result, the H abstraction channel for the HCOCl + H reaction is the dominating reaction at the whole temperature range.

IV. Summary

We presented a direct ab initio dynamics study of the thermal rate constants of two channels of the reaction of HCOCl + H. The calculated structural information, at the BHandHLYP/cc-pVDZ, MP2/cc-pVDZ, and QCISD/cc-pVDZ levels of theory, are similar to each other and are in good agreement with the available experimental data. The computed reaction enthalpies of both channels are quite close at the HL//BHandHLYP and HL//QCISD as well as QCISD(T)//BHandHLYP and QCISD(T)//QCISD levels of theory, respectively. This suggests that the BHandHLYP/cc-pVDZ and QCISD/cc-pVDZ levels of theory can provide reasonable geometric information. Furthermore, HL single-point energy refinement are needed to get more accurate energetic.

The rate constants of the reaction are evaluated using the TST, ICVT, and ICVT/SCT methods in the temperature range of 300−2500 K. The Arrhenius expressions of the calculated ICVT/SCT rate constants fitted at the HL//BHandHLYP/cc-pVDZ and HL//QCISD/cc-pVDZ levels of theory for the H abstraction channel are $k_1^{\mathrm{ICVT/SCT}}(T) = 1.16 \times 10^{-19}\ T^{2.61}\ \mathrm{e}^{(-1018.4/T)}$ and $k_1^{\mathrm{ICVT/SCT}}(T) = 1.64 \times 10^{-18}\ T^{2.25}\mathrm{e}^{(-1943.1/T)}$, and for the Cl abstraction channel are $k_2^{\mathrm{ICVT/SCT}}(T) = 1.16 \times 10^{-17}T^{1.90}\mathrm{e}^{(-3017.1/T)}$ and $k_2^{\mathrm{ICVT/SCT}}(T) = 1.85 \times 10^{-18}T^{2.12}\mathrm{e}^{(-3473.4/T)}$, respectively. The results show that the rate constants for both channels have a positive temperature dependence in the temperature range 300−2500 K. The tunneling effect is important in the H abstraction channel. The Cl abstraction channel is the minor reaction at the whole temperature range.

Consider that the orders of magnitude of the rate constants of the reactions for HCOCl with Cl, OH, and H_2O at about 300 K are about $-13 \sim -12$,[17−19] −13,[21] and −22,[20] respectively. At 300 K, the rate constant of the H abstraction channel of the title reaction is at the order of magnitude of −14 and −15 from the HL//BHandHLYP and HL//QCISD methods, respectively. Then the reaction feasibility of formyl chloride with the species in the atmosphere, mentioned above in the present study, is Cl > OH > H > H_2O.

References and Notes

(1) Prather, M. J.; Watson, R. T. *Nature* **1990**, *344*, 729.

(2) Anderson, J. G.; Toohey, D. W.; Brune, W. H. *Science* **1991**, *251*, 39.

(3) Rowland, F. S. *Ambio* **1990**, *19*, 281.

(4) Rowland, F. S. *Environ. Sci. Technol.* **1991**, *25*, 622.

(5) WMO Scientific Assessment of Stratospheric Ozone: 1989, World Meteorological Organization Global Ozone Reseach and Monitoring Project; WMO: Geneva, Switzerland, 1990; Report No. 20, Volume I.

(6) WMO Scientific Assessment of Ozone Depletion: 1991, World Meteorological Organization Global Ozone Reseach and Monitoring Project; WMO: Geneva, Switzerland, 1992; Report No. 25.

(7) McFarland, M. *Environ. Sci. Technol.* **1989**, *23*, 1203.

(8) WMO Scientific Assessment of Stratospheric Ozone: 1989, World Meteorological Organization Global Ozone Reseach and Monitoring Project; WMO: Geneva, Switzerland, 1990; Report No. 20, Volume II.

(9) Hoffman, J. S. *Ambio* **1990**, *19*, 329.

(10) Atkinson, R. Tropospheric reactions of the haloalkyl radicals from hydroxyl radical reaction with a series of alternative fluorocarbons, in Scientific Assessment of Stratospheric Ozone: 1989, World Meteorological Organization Global Ozone Reseach and Monitoring Project; WMO: Geneva, Switzerland, 1990; Report No. 20, Volume II, pp 165−205.

(11) Tuazon, E. C.; Atkinson, R.; Aschmann, S. M.; Goodman, M. A.; Winer, A. M. *Int. J. Chem. Kinet.* **1988**, *20*, 241.

(12) Sanhueza, E.; Heicklen, J. *J. Phys. Chem.* **1975**, *79*, 7.

(13) Niki, H.; Maker, P. D.; Savage, C. M.; Breitenbach, L. P.; Martinez, R. I.; Herron, J. T. *J. Phys. Chem.* **1982**, *86*, 1858.

(14) Niki, H.; Maker, P. D.; Breitenbach, L. P. *Int. J. Chem. Kinet.* **1980**, *12*, 1001.

(15) Gay, W. B.; Hanst, P. L.; Bufalini, J. J.; Noonan, R. C. *Environ. Sci. Technol.* **1976**, *10*, 58.

(16) Fantechi, G.; Jensen, N. R.; Saastad, O.; Hjorth, J.; Peeters, J. *J. Atoms. Chem.* **1998**, *31*, 247.

(17) Atkinson, R.; Baulch, D. L.; Cox, R. A.; Hampson, R. F., Jr.; Kerr, J. A.; Rossi, M. J.; Troe, J. *J. Phys. Chem. Ref. Data* **1997**, 26, 521.

(18) Catoire, V.; Lesclaux, R.; Schneider, W. F.; Wallington, T. J. *J. Phys. Chem.* **1996**, *100*, 14356.

(19) Wallington, T. J.; Hurley, M. D.; Schneider, W. F. *Chem. Phys. Lett.* **1996**, *251*, 164.

(20) Libuda, H. G.; Zabel, F.; Fink, E. H.; Becker, K. H. *J. Phys. Chem.* **1990**, *94*, 5860.

(21) Francisco, J. S. *J. Chem. Phys.* **1996**, *96*, 7597.

(22) Mora-Diez, N.; Alvarez-Idaboy, J. R.; Boyd, R. J. *J. Phys. Chem.* **2001**, *105*, 9034.

(23) Niki, H.; Maker, P. D.; Savage, C. M.; Breitenbach, L. P. *Int. J. Chem. Kinet.* **1980**, *12*, 915.

(24) Jasien, P. G. *J. Phys. Chem.* **1994**, *98*, 2859.

(25) Tyrell, J.; Lewis-Bevan, W. *J. Phys. Chem.* **1992**, *96*, 1691.

(26) Garrett, B. C.; Truhlar, D. G.; Grev, R. S.; Magnuson, A. W. *J. Phys. Chem.* **1980**, *84*, 1730.

(27) Liu, Y.-P.; Lynch, G. C.; Truong, T. N.; Lu, D.-h.; Truhlar, D. G. *J. Am. Chem. Soc.* **1993**, *115*, 2408.

(28) Lu, D.-h.; Truong, T. N.; Melissas, V. S.; Lynch, G. C.; Liu, Y.-P.; Garrett, B. C.; Steckler, R.; Isaacson, A. D.; Rai, S. N.; Hancock, G. C.; Lauderdale, J. G.; Joseph, T.; Truhlar, D. G. *Comput. Phys. Commun.* **1992**, *71*, 235.

(29) Truhlar, D. G.; Garrett, B. C.; Klippenstein, S. J. *J. Phys. Chem.* **1996**, *100*, 12771.

(30) Truong, T. N.; Truhlar, D. G. *J. Chem. Phys.* **1990**, *93*, 1761.

(31) Chuang, Y.-Y.; Corchado, J. C.; Fast, P. L.; Villa, J.; Hu, W.-P.; Liu, Y.-P.; Lynch, G. C.; Jackels, C. F.; Nguyen, K.; Gu, M. Z.; Rossi, I.; Coitino, E.; Clayton, S.; Melissas, V. S.; Lynch, B. J.; Steckler, R.; Garret, B. C.; Isaacson, A. D.; Truhlar, D. G. *POLYRATE*, version 8.2; University of Minnesota: Minneapolis, Minnesota, 1999.

(32) Becke, A. D. *J. Chem. Phys.* **1993**, *98*, 1372.

(33) Lee, C.; Yang, W.; Parr, R. G. *Phys. Rev. B* **1988**, *37*, 785.

(34) Moller, C.; Plesst, M. S. *Phys. Rev.* **1934**, *46*, 618.

(35) Pople, J. A.; Head-Gordon, M.; Raghavachari, K. *J. Chem. Phys.* **1987**, *87*, 5968.

(36))Peterson, K. A.; Woon, D. E.; Dunning, T. H. *J. Chem. Phys.* **1994**, *100*, 7410.

(37) Woon, D. E.; Dunning, T. H. *J. Chem. Phys.* **1993**, *98*, 1358.

(38) Miller, J. A.; Klippenstein, S. J. *J. Phys. Chem. A* **2003**, *107*, 2680.

(39) Frisch, M. J.; Trucks, G. W.; Schlegel, H. B.; Scuseria, G. E.; Robb, M. A.; Cheeseman, J. R.; Zakrzewski, V. G.; Montgomery, J. A., Jr.; Stratmann, R. E.; Burant, J. C.; Dapprich, S.; Millam, J. M.; Daniels, A. D.; Kudin, K. N.; Strain, M. C.; Farkas, O.; Tomasi, J.; Barone, V.; Cossi, M.; Cammi, R.; Mennucci, B.; Pomelli, C.; Adamo, C.; Clifford, S.; Ochterski, J.; Petersson, G. A.; Ayala, P. Y.; Cui, Q.; Morokuma, K.; Malick, D. K.; Rabuck, A. D.; Raghavachari, K.; Foresman, J. B.; Cioslowski, J.; Ortiz, J. V.; Stefanov, B. B.; Liu, G.; Liashenko, A.; Piskorz, P.; Komaromi, I.; Gomperts, R.; Martin, R. L.; Fox, D. J.; Keith, T.; Al-Laham, M. A.; Peng, C. Y.; Nanayakkara, A.; Gonzalez, C.; Challacombe, M.; Gill, P. M. W.; Johnson, B. G.; Chen, W.; Wong, M. W.; Andres, J. L.; Head-Gordon, M.; Replogle, E. S.; Pople, J. A. *Gaussian 98*; Gaussian, Inc.: Pittsburgh, PA, 1998.

(40) Rayez, M. T.; Rayez, J. C. *J. Phys. Chem.* **1994**, *98*, 11342.

(41) Defrees, D. J.; Levi, B. A.; Pollack, S. K.; Hehre, W. J.; Binkley, J. S.; Pople, J. A. *J. Am. Chem. Soc.* **1979**, *101*, 4085.

(42) Davis, R. W.; Gerry, M. C. L. *J. Mol. Spectrosc.* **1983**, *97*, 117.

(43) Fang, W.-H.; Liu, R.-Z. *J. Chem. Phys.* **2001**, *115*, 10431.

(44) Anand, S.; Schlegel, H. B. *J. Phys. Chem. A* **2002**, *106*, 11623.

(45) Joo, D.-L.; Laboy, J.; Kolomeisky, A.; Zhuo, Q.; Clouthier, D. J.; Chan, C. P.; Merer, A. J.; Judge, R. H. *J. Mol. Spectrosc.* **1995**, *170*, 346.

(46) Joo, D.-L.; Clouthier, D. J.; Merer, A. J. *J. Chem. Phys.* **1994**, *101*, 31.

(47) French, J. L.; Clouthier, D. J.; Chan, C. P.; Ma, E. S. F.; Lai, V. W.-M.; Merer, A. J.; Judge, R. H. *J. Mol. Spectrosc.* **1994**, *168*, 99.

(48) Fridgen, T. D.; Parnis, J. M. *J. Phys. Chem. A* **1997**, *101*, 5117.

(49) Schnockel, H.; Eberlein, R. A.; Plitt, H. S. *J. Chem. Phys.* **1992**, *97*, 4.

(50) Chen, S.-H.; Chu, L.-K.; Chen, Y.-J.; Chen, I.-C.; Lee, Y.-P. *Chem. Phys. Lett.* **2001**, *333*, 365.

(51) Pettersson, M.; Khriachtchev, L.; Jolkkonen, S.; Rasanen, M. *J. Phys. Chem. A* **1999**, *103*, 9154.

(52) *JANAF Thermechemical Tables*, 2nd ed.; National Bureau of Standards: Washington, DC, 1986; Vol. 37.

(53) Joo, D. l.; Clouthier, D. J.; Lau, B.; Merer, A. J. *J. Mol. Spectrosc.* **1993**, *161*, 123.

(54) Gonzalez, C.; Schlegel, H. B. *J. Chem. Phys.* **1989**, *90*, 2154.